

# We are IntechOpen, the world's leading publisher of Open Access books Built by scientists, for scientists

6,900

Open access books available

186,000

International authors and editors

200M

Downloads

Our authors are among the

154

Countries delivered to

TOP 1%

most cited scientists

12.2%

Contributors from top 500 universities



WEB OF SCIENCE™

Selection of our books indexed in the Book Citation Index  
in Web of Science™ Core Collection (BKCI)

Interested in publishing with us?  
Contact [book.department@intechopen.com](mailto:book.department@intechopen.com)

Numbers displayed above are based on latest data collected.  
For more information visit [www.intechopen.com](http://www.intechopen.com)



# Optimization of Spouted Bed Scale-Up by Square-Based Multiple Unit Design

Giorgio Rovero, Massimo Curti and Giuliano Cavaglià  
*Politecnico di Torino*  
*K&E Srl*  
*Italy*

## 1. Introduction

Among several configurations typical of gas-solids fluidization, spouted beds have demonstrated to be characterized by a number of advantages, namely a reduced pressure drop, a relatively lower gas flow rate, the possibility of handling particles coarser than the ones treated by bubbling fluidized beds. Additionally, significant segregation is prevented by the peculiar hydraulic structure.

Spouted beds appear to go through a revival, testified by a very recent and comprehensive book on the topic (Epstein & Grace, 2011). This renewed interest arises by implementing new concepts in scaling-up spouting contactors and devising potential applications to high temperature processes, noticeable examples being given by pyrolysis and gasification of biomass, kinetically controlled drying of moist seeds to guarantee the requested qualities and polymer upgrading processes.

## 2. Generalities on fluidization

Fluidization is a hydrodynamical regime in which a bed of solid particles is expanded and suspended by an upward fluid flow. This regime is established when the fluid velocity reaches a value corresponding to the minimum fluidization. The basic design of a fluidized unit is carried out by considering a vessel having a cross section of any shape (circular, squared or rectangular) with a perforated bottom which separates the volume holding the solids from the lower gas plenum.

Fluidized beds show a number of features which are summarized below:

- forces are in balance and there is no net force acting in the system;
- the solid particle bulk exhibits a liquid-like behaviour: the surface of the solids remains horizontal by tilting the vessel;
- if two or more vessels operating in a fluidization regime are connected, the solids reach an identical hydrostatic level;
- in the presence of a side opening under the bed surface, particles gush as a liquid flow;
- heterogeneous bodies may float or sink, depending on their actual density.

Fluidization, besides being influenced by the solid characteristics, depends on the physical properties of the fluid and its superficial velocity. When this parameter is very low, the fluid

merely percolates through the particles and no movement is induced, this condition being defined as “static bed”. By rising the flow rate, frictional forces between particles and fluid increases: when the upward component of force counterbalances the particle weight, the minimum condition to expand the bed is reached. When all the particles are suspended by the fluid, the bed can be considered in a state of “incipient fluidization” and the pressure drop through any bed section equalizes the weight of the fluid and solids in that section. By further increasing the velocity, some phenomena of instability such as “bubbling or turbulent fluidization” may occur, depending on the system geometry and particle properties. In a gas-solid system operated at high fluid velocity, gas bubbles tend to coalesce and grow in volume during their upward travel; if the bed is not wide enough, a gas bubble can take all the vessel cross section, then the solid particles are lifted as a piston, giving origin to the so-called “flat slugging”. This undesired occurrence easily happens with coarse particles as well with cohesive powders. Finally, when a critical value is reached, the velocity of the gas is high enough to transport individually or in clusters the bed particles in a “pneumatic conveying” fashion. These hydraulic regimes are schematically shown in Figure 1.

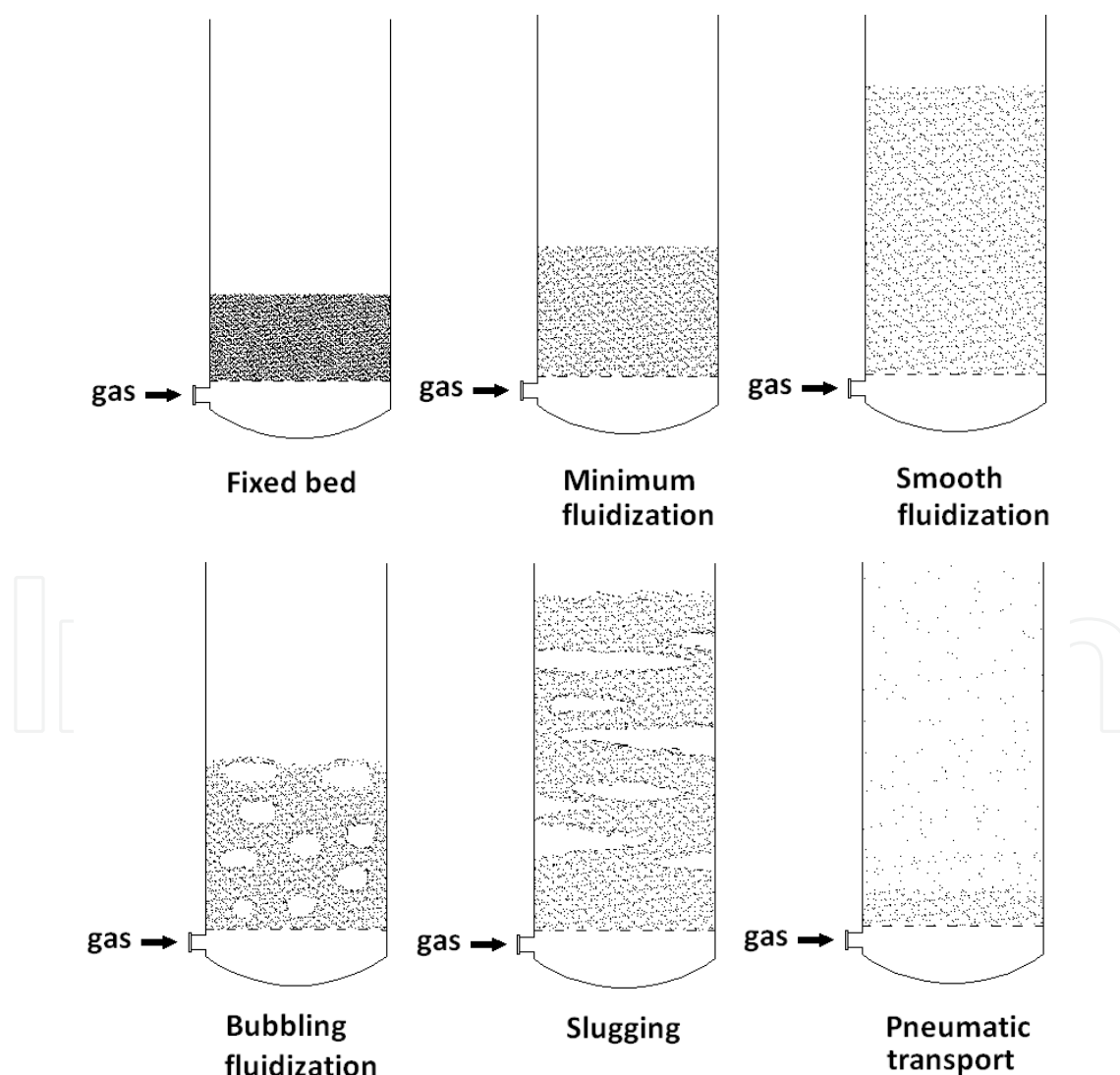


Fig. 1. Schematic representation of various fluidization regimes

In addition to properties of the fluidization medium, particle features play an essential role. A simple mapping was proposed (Geldart, 1973) to group particulate solid materials in four well-defined classes according to their hydrodynamic behaviour. To follow this categorization, Figure 2 shows the four different regions, proper of air/solids systems at ambient fluidization conditions and particles of the same shape, excluding pneumatic transport conditions.

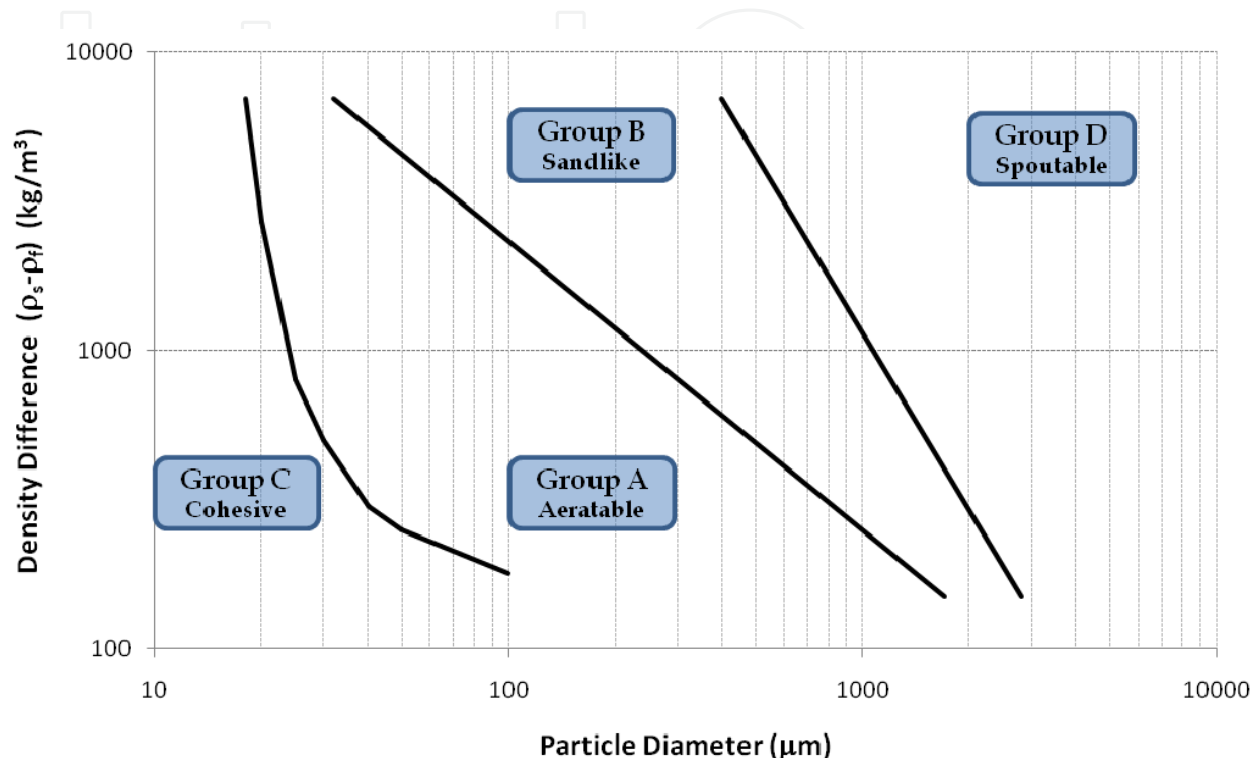


Fig. 2. Particle classification according to Geldart

The particles of the regions can be described as follows:

A type or “aeratable”: solids with small diameter and density lower than about 1400 kg/m<sup>3</sup>. The minimum fluidization velocity can be reached smoothly; then fine bubble fluidization occurs at higher gas velocities.

B type or “sandlike”: these particles are coarser than the previous ones, ranging from 40 to 1000 μm and densities from 1400 to 4000 kg/m<sup>3</sup>. A vigorous fluidization with large bubbles may be established.

C type or “cohesive”: very fine powders, with a mean diameter generally lower than 50 μm. Strong interparticle forces render fluidization difficult.

D type or “spoutable”: coarsest particles within a broad density range. These systems are characterized by a high permeability, which generates severe channelling and uneven gas distribution: the standard fluidization geometry should be modified to give origin to spouted systems.

### 3. Fluidization versus spouting

Fluidization is an operation characterized by several interesting peculiarities with desirable associated to non-optimal features. On one hand this technique guarantees a smooth and

liquid-like flow of solid particulate materials that allows continuous and easily controlled operations. The good mixing of solids provides a large thermal flywheel and secures isothermal conditions throughout the reactor. If some minor wall-effects are neglected, the solids-to-fluid relationship is independent of the vessel size, so this operation can be easily scaled up and large size operations are possible.

On the other hand, fluidization may reach conditions of instability, such as bubbling or slugging, which usually represent a situation of inefficient contact between the two phases. Moreover, in high temperature operations or with sticky particles, solids sintering or agglomeration easily occur. Finally, but not less important, fines generation, erosion of vessel, internals and pipes is a serious problem caused by the random and intense movement of particles (i.e. particle or carry over exerted by the fluid).

Mass and heat transfer related to physical and chemical reactions are kinetically limited by surface area of large particle, either when the operation occurs in the fluid phase or on the solids. In these cases fluidized systems must operate with fine particulate materials; examples are given by heterogeneous catalysis or combustion/gasification of coal fines.

For reasons intrinsic to many processes (agricultural products upgrading, agglomeration, pelletization, etc.), large particle handling is required and fluidization does not represent an optimal technology. Material comminution to reach the size required by conventional fluidization is an additional negative aspect which increases the exergetic overall process cost. A very noticeable gas rate is required to reach fluidization of large particles, which often far exceeds the amount required for the physical or chemical operation considered. It should also be noted that fluidized systems are operated at a gas rate double or triple with respect to the minimum fluidization velocity to confer the system adequate mixing and avoid any dead zone. In conclusion, fluidization appears an interesting operation thanks to an easy scale-up, though its extensive feature (large gas flow rate need) as well as its intensive characteristics (random fluid-to-particle hydraulic interaction) counterbalance its favourable aspects to some extent.

A spouted bed can be realized by replacing the perforated plate distributor typical of a standard fluidized bed with a simple orifice, either located in the central position of a flat bottom or at the apex of a bottom cone, whose profile helps the solids circulation and avoids stagnant zones. Examples of non-axial orifices appear in the scientific literature, too. The fluidizing gas enters the system at a high velocity, generates a cavity which protrudes upward through the "spout", which, having an almost cylindrical shape, can be characterized by its spout diameter value  $D_s$ . When the gas flow rate is large enough, the spout reaches the bed surface and forms a "fountain" of particles in the freeboard. The fountain can be more or less developed depending on the gas rate and the overall system features. After falling on the bed surface, the solids continue their downward travel in the "annulus" surrounding the spout and reach different depths before being recaptured into the spout. The dual hydrodynamics, good mixing in spout and fountain and piston flow in the peripheral annulus with alternated high and slow interphase transfer, in the spout and in the annulus respectively, makes spouted beds unique reactors.

Consequently, spouted beds offer very peculiar features, which can be summarized as:

- very regular circulation of particles and absence of dead zones;

- reduced pressure drop and lower gas flow rate required to attain solids motion with respect to the minimum fluidization velocity, this result being possible as the gas transfers its momentum to a limited portion of solids constituting the whole bed;
- wide range of operating conditions starting from a value slightly exceeding the minimum spouting velocity ;
- possibility of handling coarse particles having a wide size range and morphology.

#### 4. Spouted beds

The term “Spouted Bed” was coined with an early work carried out at the National Research Council of Canada by (Gishler & Mathur, 1954). A comprehensive book by (Mathur & Epstein, 1974) provided a systematic summary of the scientific work done in the years. Very recently (Epstein & Grace, 2011) the most advanced knowledge in the field has been updated.

Spouted beds were originally developed as an alternative method of drying moist seeds needing a prompt and effective processing. Sooner the interest in spouted beds grew and their application included coal gasification and combustion, pyrolysis of coal and oil shale, solid blending, nuclear particle coating, cooling and granulation as well as polymer crystallization and solid state polymerization processes. Fundamental studies were carried out to establish design correlations, the performance of spouted beds as chemical reactors, motion patterns and segregation of solids, gas distribution within the complex hydrodynamics.

Some additional improvement in the gas-to-solids contacting can be provided by independently aerating the annulus, thus generating the so-called “Spout-fluid Beds” (Chatterjee, 1970). Again, a perforated draft-tube can be placed to surround the spout, thus contributing in terms of stability and operational flexibility (Grbavčić et al., 1982).

Most studies were carried out in plain cylindrical geometries, either full sectional, half sectional or even in a reduced angular section of a cylinder in order to explore scale-up possibilities. In any case adding a flat transparent wall has been demonstrated to interfere to a moderate extent with the solids trajectory vectors within the annulus (Rovero et al., 1985) while does not affect the measurement of the fundamental parameters of spouted beds ( $U_{ms}$ ,  $H_m$ ,  $D_s$ ). A limited number of examples consider multiple spouting, either in parallel or in series, squared and rectangular cross sections (Mathur & Epstein, 1974).

#### 5. Design bases

A typical spouted bed scheme is given in Figure 3. This representation depicts the gas inlet and outlet, the upward movement of solids in the spout, their trajectories in the fountain and the subsequent descent in the annulus to reach the spout again at depths which depends on the path-lines originated by the landing position on the bed surface. The particle holdup can be loaded batchwise or, alternatively, in a continuous mode. The latter option depends on process requirements, nevertheless a continuous solids renewal in no way alters the above features. A proper solids feeding should minimize bypass towards the discharge port; in this view a direct feeding over the bed surface appears the best option to guarantee at least one circulation loop in the annulus to all the particles. A direct distributed feed over the fountain is required only in case of particles with high tendency to stick.



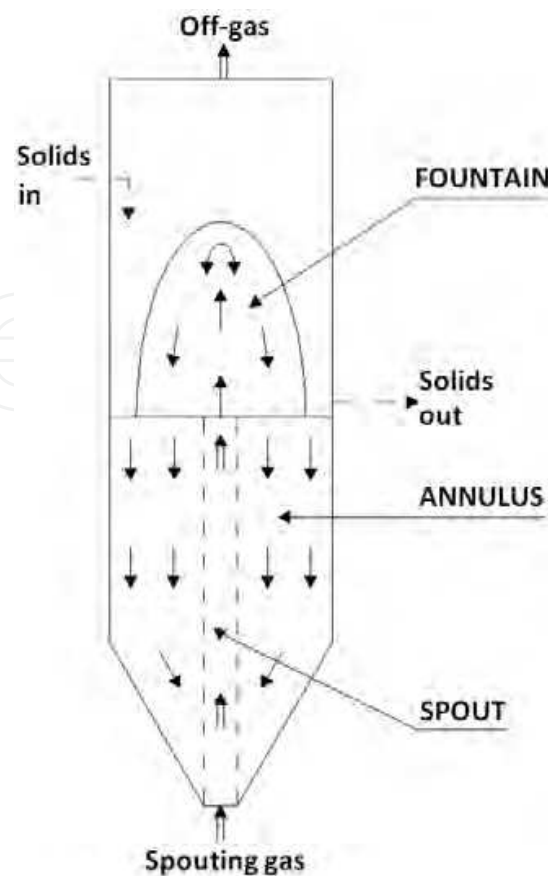


Fig. 3. Schematic of a spouted bed

The solids discharge from continuous operations is generally carried out with an overflow port, unless special process control is required. This case may be given by coating processes, where the total bed surface area should be controlled. In this case a submerged port preferentially discharges coarse material, due to local segregation mechanisms (Piccinini, 1980), while the entire spouted bed retains good mixing capacity, which can be regulated by the fountain action.

The gas flow distribution between spout and annulus is completely independent whether the solids are batch or continuously fed: part of the gas progressively percolates from the spout into the annulus by moving toward higher elevations in the bed of particles. In case of a bed of sufficient height the gas in the annulus may reach a superficial velocity close to the minimum fluidization velocity of the solids. In this event the annulus is prone to collapse into the spout, thus defining the “maximum spoutable bed depth, or  $H_m$ ”. This parameter represents one of the fundamental criteria to design a spouted bed unit (Mathur & Epstein, 1974);  $H_m$  depends on vessel geometry, fluid and particle properties.

The second fundamental parameter is given by the minimum rate of gas required to maintain the system spouting, the so-called “minimum spouting velocity, or  $U_{ms}$ ”. This operating factor can be either determined by an experimental procedure (as described in Figure 10) or can be calculated by the existing correlations.

A spouted bed, thanks to its flexibility, can be operated with a wide range of solids load to fill part or all the cone (“conical spouted beds”), or otherwise to engage also the upper portion of

the vessel ("cylindrical spouted beds"). In both cases the conical included angle is in the range of 60 to 90°; by further diminishing the angle instability in solid circulation might occur, while increasing excessively the angle decreases solids circulation at the base. A gross criterion that distinguishes conical and cylindrical spouted beds can be given considering the type of reaction to carry out: when solid phase undergoes a fast surface transformation, the optimum residence time of the gaseous phase is very short. This condition is satisfied by shallow beds as in the case of catalytic polymerization or coal gasification and pyrolysis. When the reaction is controlled by heat or mass transfer, the gas-solid contact must be adjusted with a deeper bed configuration as in drying, coating, solid phase polymerization, etc..

Thanks to this flexibility, the mean residence time of the solids in continuous operations can be regulated by optimizing the solids hold-up in a single vessel, which gives origin to a well mixed unit, or otherwise it is possible to conceive a cascade of several units to have a system approaching a plug flow. In the latter case square based units can have a number of advantages over a conventional cylindrical geometry. Specifically, the construction is cheaper, more compact and the heat dissipation toward the outside lower. Some scientific aspects remain open though: the design correlations that should be validated, the stability of multiple units proved both during the start-up and at steady state conditions and the possibility of fully predicting the solids residence time distribution as a function of geometry and number of stages.

## 6. Spouting regime

Stable spouting can be obtained by satisfying two hydrodynamic requirements: 1) the bed depth must be lower than the  $H_m$  value and 2) the gas flow rate has to exceed  $U_{ms}$ . From an initial condition of a static bed with a nil gas flow, by increasing the gas flow a certain pressure drop is built up through the bed of particles. The graph given in Figure 4 describes this hydrodynamic evolution, which implies a pressure drop/flow rate hysteresis between an increasing flow and the reverse situation. The hysteresis is caused by different packing conditions of the bed particles, that expand to attain a loose state once a spouting condition is reached. Starting from the static bed condition denoted by A, the pressure drop increases with the fluid velocity and reaches a maximum pressure drop ( $\Delta P_M$  at B). With an additional increase of the gas velocity, the bed displays a moderate progressive expansion and a corresponding decrease of pressure drop to reach C. Finally an abrupt spouting leads to a sudden decrease of pressure drop which stabilizes at an nearly constant value (D), which is maintained in all the operating range of gas rate. This situation represents a stable spouting. In case of fluid velocity decrease, the pressure drop remains constant down to the spout collapse (E), which compacts the system to some extent and the pressure drop increases again to F, giving origin to the afore mentioned hysteresis. The minimum spouting velocity is recorded at E.

The whole system hydrodynamics is given by knowing  $\Delta P_M$ ,  $U_{ms}$ ,  $\Delta P_s$  and the  $U/U_{ms}$  ratio chosen for a stable spouting. A recent paper has compared data obtained in the mentioned 0.35 m side square-base unit to the existing literature correlations (Beltramo et al., 2009). The design data for the blower are  $\Delta P_s$  and  $U$ , while the maximum pressure drop and the relative transitory flow rate can be easily generated by a side capacitive device, to be used at the start-up only. It is important knowing that the hydrodynamic transient can be as short as a few seconds, so that the capacitive device can be designed with a characteristic time shorter than a fraction of a minute. In this view, the timing of a spouting process onset is quantified in Figure 15.



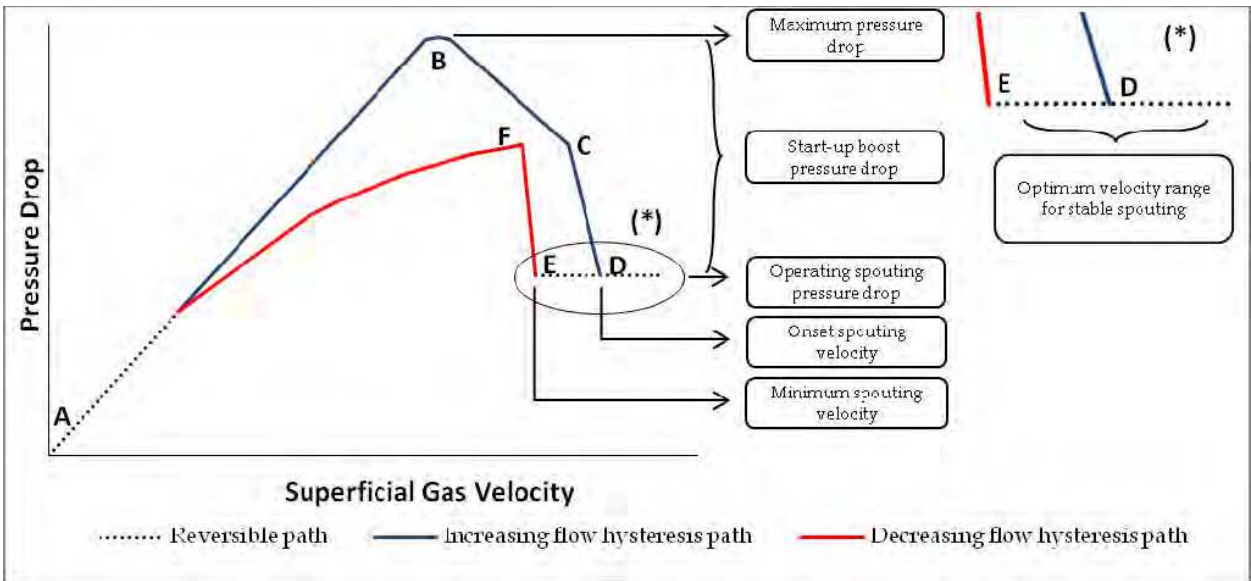


Fig. 4. Hydrodynamic diagram for spouting onset

Figure 5 displays a sequence of pictures that show the spout onset from the initial cavity generation (A) to the full spouting. The third picture qualitatively corresponds to the point B in Figure 4, the fourth picture shows the rapid sequence between C and D, while the last picture may describe any point in the interval E-D, or over.

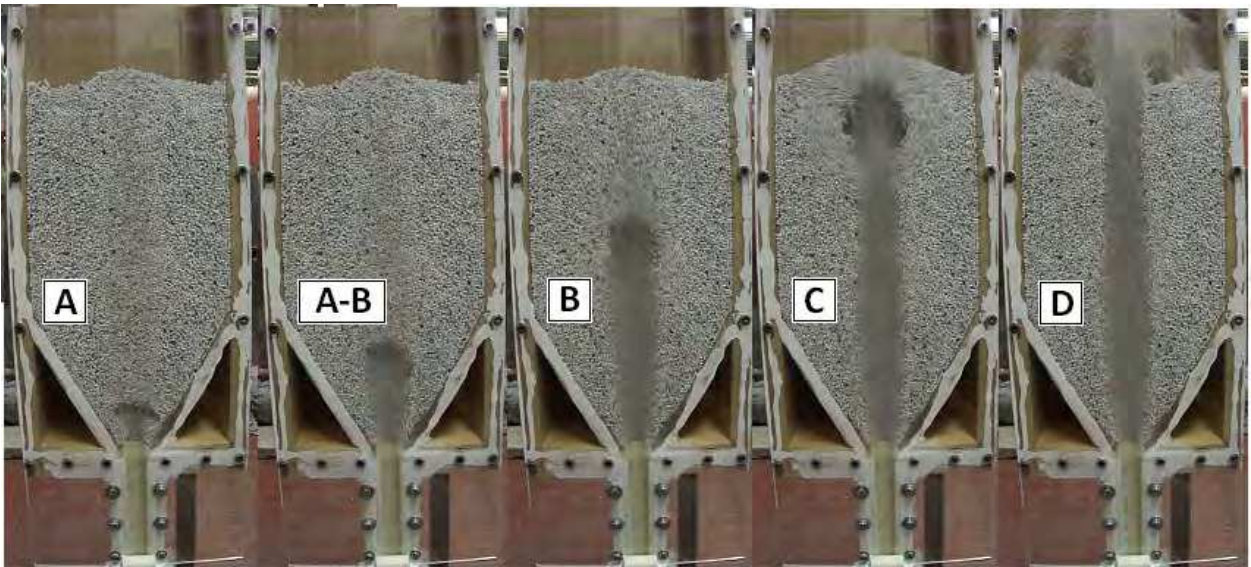


Fig. 5. Photographic sequence of the evolution of a spouting process performed in a squared-based half sectional 0.2 m side unit

7. Scale-up

Due to the peculiarities of spouted beds, their application to industrial processes requires a sound experience and a clear vision of their hydrodynamics since scale-up from laboratory experience is required. A summary of industrial implementations appears in the recent book

on spouted beds by (Epstein & Grace, 2011) together with general criteria, though the issue remains open.

Scaling-up a spouted and spout-fluid beds can be tackled according two approaches:

1. increasing the size of a single unit, or
2. repeating side by side several units.

Both routes must be discussed in terms of advantages and drawbacks. The first approach implies a simple geometry and mechanic construction: some doubts arise on the validity of the existing correlations and the overall hydrodynamics in the unit (gas distribution between spout and annulus, solids circulation, etc.). The use of the existing correlations up to a unit diameter ( $D_c$ ) of about 0.6 m is generally thought fully safe. If a continuous operation is considered, this arrangement gives the solid particulate material a well-mixed behaviour with a broad distribution of particle residence time at the exit of the unit.

Conversely, if a sequence of multiple beds is realized, achieving a fully independence of the units becomes the fundamental goal. In other words a non-interfering system must be designed, so that it is up to the operator decide which unit to start-up or shut-down first according to process needs. Due to the complexity of a multiple system each unit must mandatorily replicate the foreseen behaviour of the basic component. In this case, the residence time distribution of the solids approaches closely a plug flow to meet most process requirements.

Design geometry and regulation criteria are thoroughly discussed in the continuation of this chapter. The design and the construction of a multiple unit implies a careful geometrical optimization to minimize heat loss, investment and operating costs, assure a straightforward start-up, guarantee stability and process performance. According to this key requirement, squared-based units could replace a standard cylindrical section geometry, according to an account presented in literature (Beltramo et al., 2009). A correlation between cylindrical and square-based units is also needed.

## 8. Experimentation on single and multiple square-based units

This chapter describes a systematic experimentation in a 0.13, 0.20 and 0.35 m side units to correlate the hydrodynamics of square-based spouted beds to the one of a corresponding cylindrical units and define the optimal geometrical configuration to assure solids circulation and transfer to downstream modules when multiple spouted beds in series are considered. The square-based experimental modules were made of wood with a frontal Perspex wall or of AISI 316 SS with a tempered glass window, depending on whether the apparatus had to be operated at room or higher temperatures. A 0.15 m ID cylindrical unit was also used for data comparison. Table 1 provides more geometrical details of the spouted beds. All bases, either frustum shaped or conical were characterized by an included angle of 60°. The spout orifice extended up of 1 mm over the base to improve solids circulation at the bed bottom, according to suggestion existing in the literature. The vessels were 1.5 m or 2 m high to allow the measurement of the maximum spoutable bed depth for all the solids tested.

The tests were carried out with several materials to cover a sufficient range of parameters, as they appear in Table 2.

Module type:	Section	Side (m)	Diameter (m)	Equivalent diameter (m)	Height of the unit (m)	Cone / Pyramid angle (deg)
L-13	squared	0.13	-	0.15	1.50	60
D-15	cylindrical	-	0.15	0.15	1.50	60
L-20	squared	0.20	-	0.23	2.00	60
L-35	squared	0.35	-	0.40	2.50	60
half L-20	rectangular	0.20	-	-	2.00	60

Table 1. Geometrical characteristics of spouted test apparatuses

Material	Equivalent mean diameter (mm)	Density (kg/m³)	Sphericity	Repose angle (deg)
PET chips	3.04	1336	0.87	35
Turnip seeds	1.50	1081	1.00	27
Corn	7.82	1186	0.80	27
Soya beans	7.23	1144	0.99	29
Sunflower seeds	6.16	696	0.87	37

Table 2. Physical properties of the particulate material used



Fig. 6. Materials used in the tests

The experimental equipment was composed of several units, whose pictures are given in Figure 7A and 7B. Depending on the flow rate required, air as spouting medium was either provided by two volumetric compressors (total flow rate of about 250 Nm<sup>3</sup>/hr) or from a blower (flow rate of 350 Nm<sup>3</sup>/hr). The air flow was cooled through a corrugated pipe heat exchanger to guarantee spouting at a constant room temperature. Two rotameters were used to meter the flow together with gauge pressure recording.

The experimental strategy was directed both to run batch experiments in a single vessel to assess the fundamental spouting parameters ( $H_m$ ,  $U_{ms}$ , a stable  $U/U_{ms}$  ratio), as well as



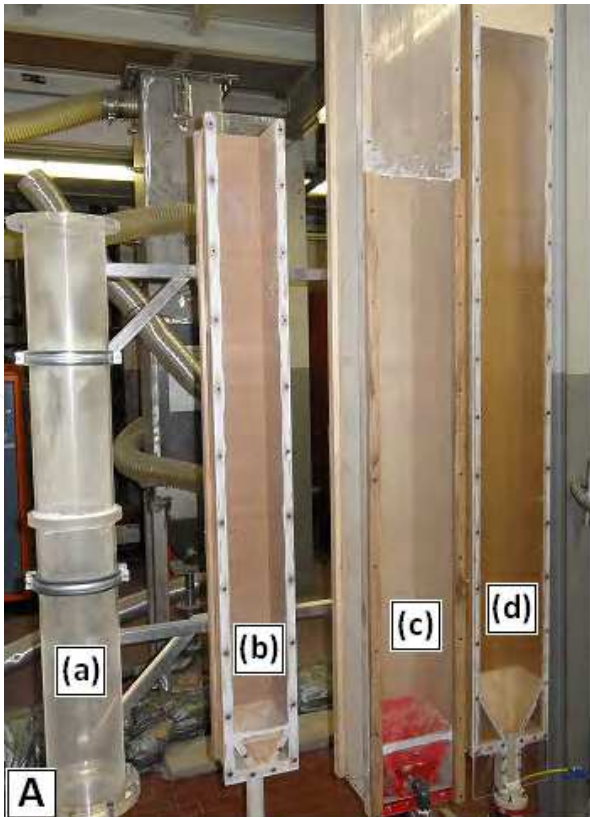


Fig. 7A. See from left to right: a) 0.15 m ID cylindrical Perspex spouted bed vessel, b) 0.13 m side square-based wooden unit; equivalent to a), c) 0.20 m side square-based wooden unit and d) half-sectional 0.20x0.10 m<sup>2</sup> square-based wooden unit.



Fig. 7B. 0.35 m side square-based AISI 316 SS unit with tempered glass frontal window.

optimize the geometrical spouted bed features (details of the base, orifice diameter, particle traps at the gas exit, etc.). Additionally, cylindrical and square-based vessels were comparatively tested.

Continuously operating experiments were directed to design the geometry of internals required to guarantee easy start-up, spouting stability in a multiple stage unit, discharge facilities to minimize “off-spec” products, adequate solids transfer from the feeding port, through the inter-stage weir, to the final overflow discharge.

Figure 8A provides the schematic view of the spouted bed assemblage of D-15, L-13, L-20, half-L-20 and L-35 units for batchwise measurements of the fundamental operating

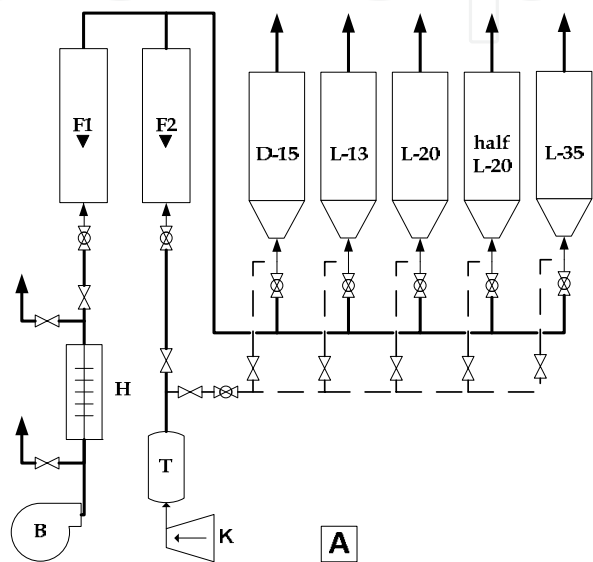


Fig. 8A. Schematic of the spouted bed assemblage for batch measurements of operating parameters (see legend in the below Fig. 8B)

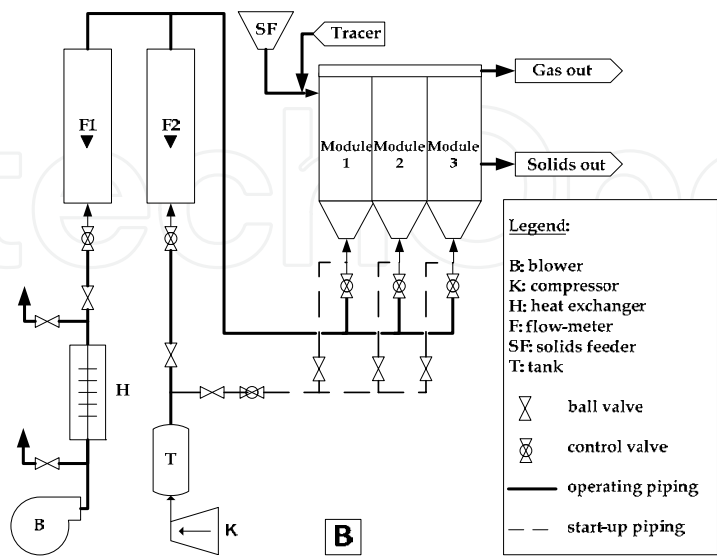


Fig. 8B. Schematic of the three module spouted bed for continuous hydrodynamic measurements

parameters characteristic ( $H_m$ ,  $U_{ms}$ ,  $D_s$ , mean particle velocity in the annulus, volume of spout and fountain). Figure 8B shows the scheme of the three cell equipment used to optimize geometry of internals, overall structure, effect of continuous solids feeding and residence time distribution of the solid phase.

8.1 Batch unit tests

The hydrodynamic behaviour of a square-based spouted beds was evaluated by exploring a wide range of conditions, from a bed depth corresponding to the frustum height to the maximum spoutable bed depth by operating with all the material shown in Figure 6. A reasonable ample scale-up factor (in excess of 7) was considered by running four square-based units of 0.13, 0.20 and 0.35 m side. Moreover the 0.13 m side unit was compared to the equivalent 0.15 m ID cylindrical unit to identify any difference in terms of  $U_{ms}$  and  $H_m$  and then validate the applicability of the existing correlations to the non-standard square-based geometry.

8.1.1 Maximum spoutable bed depth

The maximum spoutable bed depth is measured by progressively adding solid granulated material in the vessel and verifying that a stable spout could be formed. Some difficult transition may be encountered at  $H \approx H_m$  to make the spouting process neatly evolve from an internal spout to an external well-formed one; in these cases some subjective uncertainty may be left in the measurements. In this case visualization in half-column can be useful (see the photographs of Fig.14).

Table 3 presents the experimental results obtained in two equivalent units, namely the cylindrical 0.15 m ID column (D-15) and the 0.13 m side square-based vessel (L-13); additionally, the larger L-20 vessel provided data useful for scale-up and validation of existing correlations. The test results show good and consistent agreement with the predictions given by literature equations (Malek & Lu, 1965; McNab & Bridgwater, 1977).

	D-15	L-13	L-20
Material	$H_m$ , m	$H_m$ , m	$H_m$ , m
PET chips	0.69	0.65	1.26
Turnip seeds	0.84	0.85	1.44
Corn	0.41	0.46	0.98
Soya beans	0.37	0.36	0.65
Sunflower seeds	0.68	0.69	1.48

Table 3. Experimental values of the maximum spoutable bed depth  $H_m$  in the 0.13 m side square-based unit (L-13), in the 0.20 m side square-based unit (L-20) and in the 0.15 m ID cylindrical spouted bed (D-15).

Another interesting result derived from the comparison of the D-15 and L-13 units; the maximum spoutable bed depth values are very close for the same particles and identical orifice, so it allows us to assume that this fluid dynamic parameter does not depend on the cross section geometry. For this reason several correlations predicting  $H_m$  can be



indifferently applied to both geometries. The herein below Malek-Lu (derived in SI units) and McNab-Bridgwater equations, among others, were compared with the experimental results, as it appears in Figure 9. The agreement can be defined fully satisfactory.

Malek-Lu equation:

$$\frac{H_M}{D_C} = 418 \cdot \left( \frac{D_C}{d_p} \right)^{0.75} \cdot \left( \frac{D_C}{d_i} \right)^{0.40} \cdot \left( \frac{\lambda^2}{\rho_s^{1.2}} \right) \quad (1)$$

McNab-Bridgwater equation:

$$H_M = \frac{D_C^2}{d_p} \cdot \left( \frac{D_C}{d_i} \right)^{2/3} \cdot \frac{700}{Ar} \left( \sqrt{1 + 35.9 \cdot 10^{-6} \cdot Ar} - 1 \right)^2 \quad (2)$$

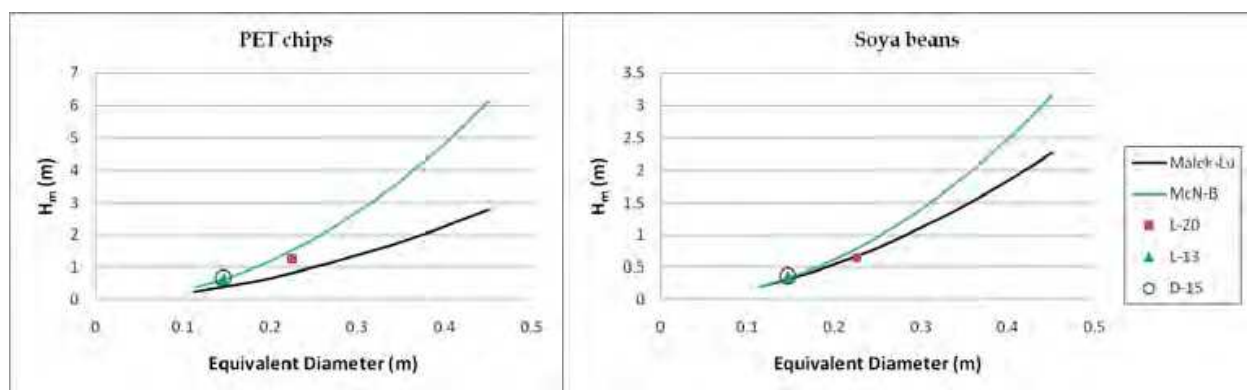


Fig. 9. Comparison of experimental data obtained in square-based and cylindrical units with literature correlations

### 8.1.2 Minimum spouting velocity

As given in the hydrodynamic diagram of Figure 4, the minimum spouting velocity  $U_{ms}$  represents the superficial velocity in the vessel below which spouting does not occur. Aiming to work in a stable situation, good practice suggests to moderately exceed this value by defining an operating spouting regime given by  $U/U_{ms} > \text{about } 1.05$ , which is the measure of a very modest excess of gas with respect to the minimum spouting condition. It is worthwhile noting that this value can be further reduced if the spouted bed approaches its maximum spoutable bed depth  $H_m$ , as the below Figure 10 diagram indicates. The onset spouting and minimum spouting velocities approach as  $H$  is closer to  $H_m$ . This occurrence also indicates that passing from a submerged to an external spouting is progressively easier as  $H_m$  is approached, since the bed of particles is already highly expanded by a very high gas rate (pictures on Figure 14 represent this case). Consistently, these operating conditions generate hydrodynamic diagrams with a much less pronounced hysteresis, as given in a recent paper (Beltramo et al., 2009). To predict the minimum spouting velocity in multiple cell systems an empirical correlation was proposed (Murthy and Singh, 1994). By observing carefully the type of plots appearing in Figure 10, it is possible to note that the maximum bed depth can be inferred from the overlapping of the two curves. This remarkable experimental statement (based on hydrodynamic data) may offer an interesting alternative

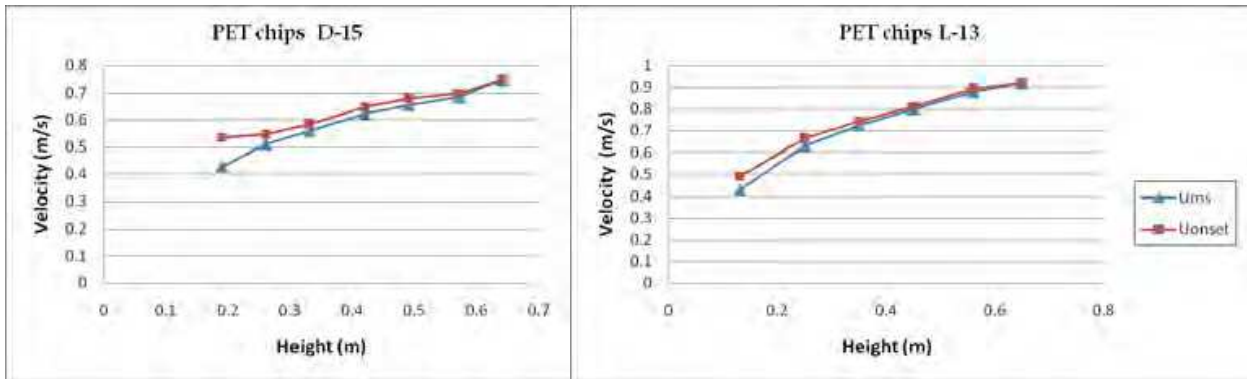


Fig. 10. Onset and minimum spouting velocities vs. bed depth

to direct observations, which are ambiguous in some instances due to bed instability as  $H_m$  is approached. Moreover careful extrapolation of the  $U_{ms}$  and  $U_{onset}$  curves to detect their intersection is a possible method to estimate  $H_m$  when the experimental conditions are not suitable for a complete direct measurement.

8.2 Continuously operating multiple units

A continuously operating unit was tested to devise a guideline to design, start-up, gain in stability and proper hydrodynamics in multiple square-based spouted beds.

A picture of the rig is present in Figure 11A, while a 3D scheme of the same unit is shown below, see Figure 11B.



Fig. 11A. Picture of the three-module experimental rig.

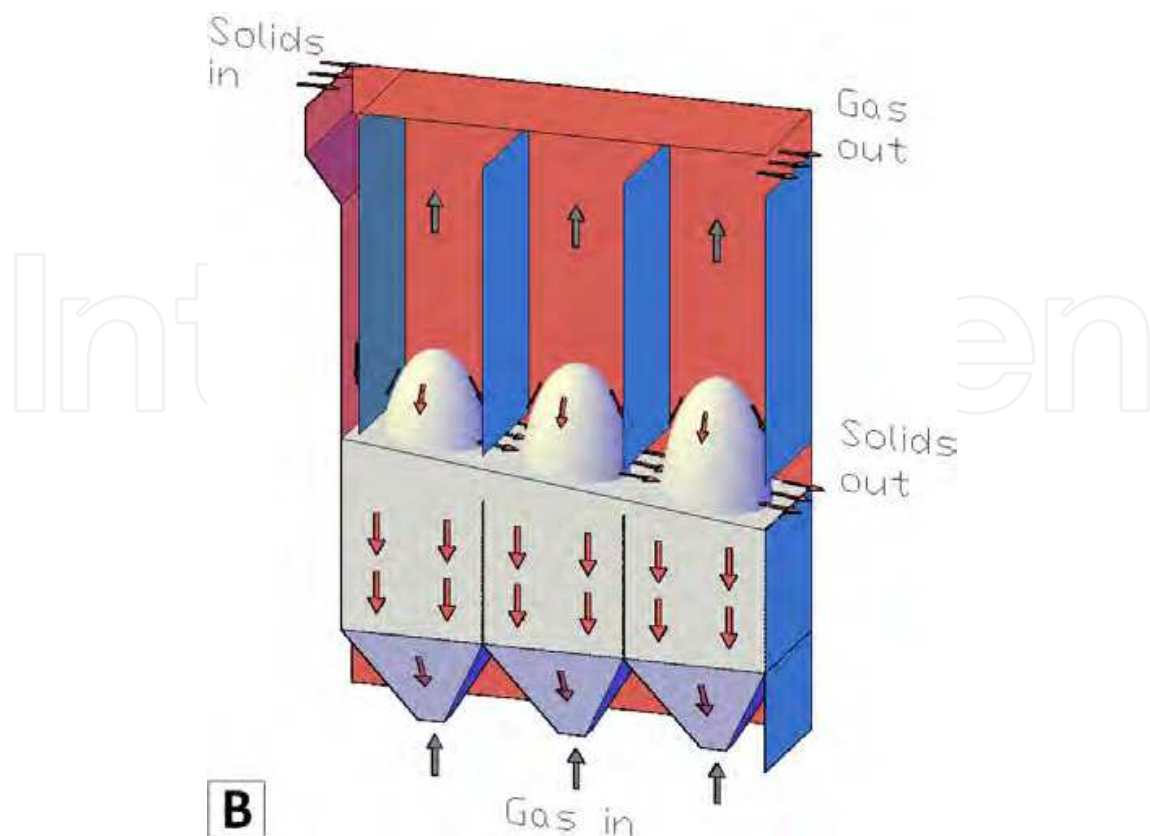


Fig. 11B. 3D diagram of the same continuously operating unit with a horizontal layout of stages

Designing a multiple spouted bed system does not represent a “black art”, though may be more complex than other gas/solids contactors. In particular the following design aspects were focused in this project:

- diverting baffle at solids inlet,
- fountain height regulators,
- freeboard baffles between units,
- submerged baffles between units,
- overall layout of a multiple spouting unit

The following paragraphs illustrate the progressive tuning of a multiple stage spouted bed up to achieve safe know-how and run continuous operations.

### 8.2.1 Solids inlet design

Solid particles were stored in an elevated drum, from which they could flow by gravity, being metered by a rotary valve, a screw feeder or a simple calibrated orifice. The particles were distributed along one entire side of the spouted bed, addressed down by a vertical baffle protruding to a small distance from the bed free surface. This simple device avoided any solids bypass promoted by the fountain. Residence time distribution measurements quantified a bypass as high as about 20% of the total flow rate, in case of baffle absence. The elevation of the baffle over the bed may require some regulation, depending on solids feed rate.

### 8.2.2 Fountain height regulators

A spouted bed fountain can be defined underdeveloped, developed or overdeveloped, depending on whether its geometrical margins reach the side of the spouting vessel. Since the volumetric solids circulation through the spout/fountain system can be estimated to range to a few percents of the spouting gas flow rate, the fountain alone can pour very noticeable flows of material onto contiguous stages; then, its action should be limited by some mechanical device to restrain its hydrodynamic effect. Some devices, the so-called “Chinese hats” were presented in the sector literature (Mathur & Epstein, 1974) and tested in this unit. The experimental output was entirely disappointing, as these regulators failed in sufficiently defining the fountain shape, acted as a target for the particles propelled by the spout and interfered hydrodynamically with the gas flow in the freeboard, either when they were made of solid steel plates or wire mesh screen. To conclude, these devices are not advisable as internals in multistage spouted beds.

### 8.2.3 Freeboard baffles between stages

Each stage was segregated from its adjacent ones by side vertical baffles protruding down from the vessel top to a very short elevation over the bed free surface. The gap left had to assure solids flow only, depending on the continuous throughput rate; this gap between the submerged and the freeboard baffles has to be regulated to allow solids transfer by overflow, with restricted particle bounces from the fountain. Also bypass was minimized by this precaution. These flat and inexpensive devices were chosen to completely separate the freeboard into as many stage as the spouted bed design required. As a result, the action of each fountain (independently of its shape, thus gaining in spouting regime flexibility) was limited to its own stage. The use of these simple baffle repartition was observed to be fundamental for minimizing any interference between stages and enormously gain in stability.

### 8.2.4 Submerged baffles between stages

In principle, according to the fundamentals of fluidization, a multiple orifice spouted bed does not require a repartition between the annuluses. This consideration is also compatible with the particle vertical streamlines and the side-to-side homogeneous percolation of gas from a spout into the corresponding annulus. This assessment can be fully accepted when the system is operated batchwise and no net solids flow from one stage to the downstream one has to be steadily maintained. Practical reasons (easy start-up, spouting stability over time, independent gas flow rate regulation in each spouting module) have demonstrated that submerged baffles greatly help in defining the solids holdup in each stage. The separation of contiguous annular regions contributes in properly distributing the gas rate and giving origin to fully independent spouts. Conversely, if the holdup of solids is out of control, all the system stability may be affected.

### 8.2.5 Overall layout of a multiple spouting unit

In the recent past, in the frame of industrialization of a novel patented process for polyethylene terephthalate solid state polymerization (Cavaglià, 2003), a unit was conceived as a series of  $n$ -fluid beds (where  $n > 5$ ), operated either in turbulent fluidization or in

spouting regime, where polyester beads with low intrinsic viscosity are heated-up and solid reacted in one equipment. A sextuple spouting demonstration unit was then built and operated as a prototype equipment for PET chips upgrading (Beltramo et al., 2009). The six modules were placed at identical elevation and positioned according to a 2x3 layout; the solids moved following a chicane path without being hindered by any internal repartition. The multiple spouted bed appeared advantageous in term of heat transfer efficiency (higher gas temperature at the inlet, thanks to a very short contact time between gas and heat sensitive solids) and generated good property polymers. However, the overall operation was troublesome because of difficult control on solids holdup and gas flow rate regulation. From that study sound design hypotheses were drawn to construct the experimental rig appearing in Figure 11A, whose main difference with respect to the previous industrial equipment consists in the possibility of positioning each stage at the desired elevation to facilitate the solids overflow to the downstream stage, as represented in the schematic of Figure 12. The final version of this experimental rig had the possibility of testing all the internals described above.

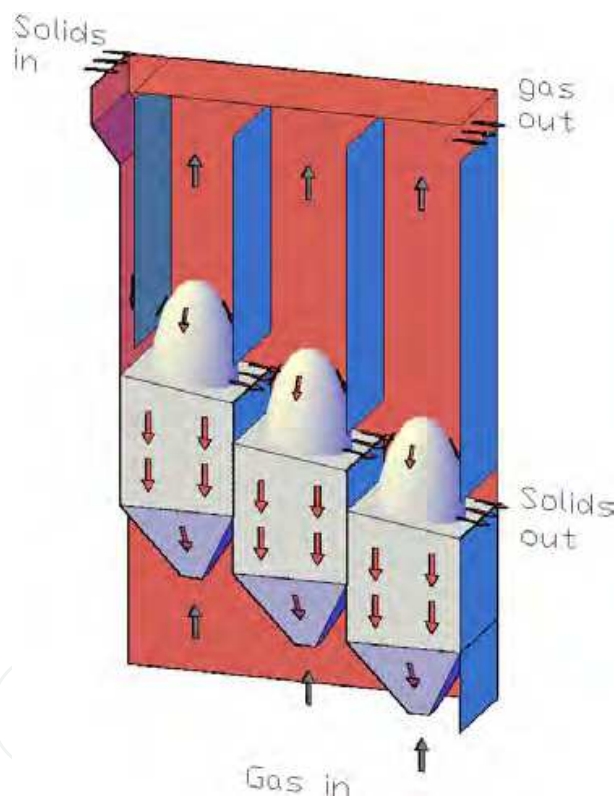


Fig. 12. 3D diagram of a continuously operating unit with a sloped layout of stages

The difference of level between units suitable for continuous and stable operations was evaluated both by running specific tests and by comparing these results against a simple correlation originated by estimating the angle of internal friction of the solids used in the experiments. The tests performed in the triple spouted bed unit aimed at devising the effect of increasing solids feed rates on bulk mass transfer from stage to stage, by measuring the angle of the bed surface with respect to the horizontal level, as well as the effectiveness of the internal baffle positioning. Figure 13 shows three different operating conditions at a mean (snapshot A), corresponding to a mean particle total residence time  $\tau = 13.5$  min), high



(snapshot B),  $\tau = 4.5$  min) solid rates and at a solids throughput far exceeding the nominal system capacity, as required by any foreseen process (snapshot C),  $\tau = 2.5$  min). The bed free surface slant increased to a maximum slope (about  $15^\circ$ , as a mean value between inlet and overflow sides) by increasing the flow rate. This angle is in the range of  $1/2$  to  $1/3$  of the solids repose angle, which can be measured following literature recommendation (Metcalf, 1965-66). By further enhancing the feed rate, the downcomer flooded unless further raised. The hydrodynamic slope that builds up at the bed surface caused the first stage to work with a solids depth quite higher with respect the last one, this difference increasing with the number of stages. It follows that the fluid dynamic control was much trickier and the overall spouting stability impaired.



Fig. 13. Continuous operation in the three-module 0.20 m side spouted bed: - - - ideal solids free surface; — actual solids surface at various solids flow rates: a) 2 kg/min, b) 6 kg/min and c) 10 kg/min, as given in the scheme of Fig. 11 B

This geometrical limitation was overcome by setting each bed at a minimum difference of level equal to:

$$\Delta H = D_c \tan \alpha \quad (3)$$

where  $\alpha$  is the angle formed by the actual solids surface with the horizontal level.

A rule of thumb suggests to determine the progressive vertical distance between adjacent spouted beds at:

$$\Delta H = 0.5 D_c \quad (4)$$

which, compared to the output of Eq. (3), leaves a safe operating margin.

As a conclusion, stable operations in a multiple square-based spouted beds require three types of flat internal baffles: one for properly addressing the solids feed to the bed surface, intermediate baffles in the freeboard to confine each fountain action, submerged baffles, each of them setting the solids overflow level from the upstream to the downstream stage. A non-interfering condition between stages was provided by generating a sloped cascade of independent spouting units.

### 8.3 Half-sectional spouted bed tests

A rig corresponding to half of the  $0.20 \times 0.20$  m<sup>2</sup> spouted bed was built to represent a vertical section of the full unit. The axial sectioning included the orifice, the pyramid frustum and the constant cross section sector, thus originating a  $0.20 \times 0.10$  m<sup>2</sup> column. A



flat Perspex wall allowed a direct internal vision of spout, annulus and fountain, as already given in Figure 5.

Specific tests were carried out to demonstrate the close correspondence between data ( $H_m$  and  $U_{ms}$ ) obtained in full and half-sectional columns. Approaching the maximum bed depth an underdeveloped and stable fountain was obtained with  $U = 1.01 U_{ms}$  (Figure 14 a)). Other runs highlighted a relevant bed expansion surmounting a submerged spout when the bed slightly exceeded the maximum bed depth (Figure 14 b)). Identical conditions also revealed occasional instability identified by a submerged wandering spout and some upper slugging, see Figure 14 c)).



Fig. 14. Half sectional column tests at H: a) external spout and fountain formation at  $H \approx 0.95 H_m$ , b) submerged spouting at  $H \approx 1.05 H_m$  c) spouting instability with spout wandering at  $H \approx 1.05 H_m$

Half-sectional units are suitable to measure particle cycle time, define solids streamlines, as well as visualize, at proper frame frequency, zones characterized by a high mixing degree. As far as the downward particle velocities are concerned, the considerations presented in the literature were taken into account, though obtained in semicylindrical vessels (Rovero et al., 1985). Figure 15 shows a sequence of snapshots which make visible the progressive motion of a tracer layer deposited on a fixed bed before starting the spouting process (first image). The second snapshot indicates that the tracer particles have maintained their position ahead of an external spout to be formed. The third and fourth images indicate that particles move in the fountain in a piston flow fashion: then, local trajectories, their envelope (i.e. streamlines) and individual particle velocities can be defined. A minor portion of tracer only has been captured by the spout in the travel along the constant cross section of the

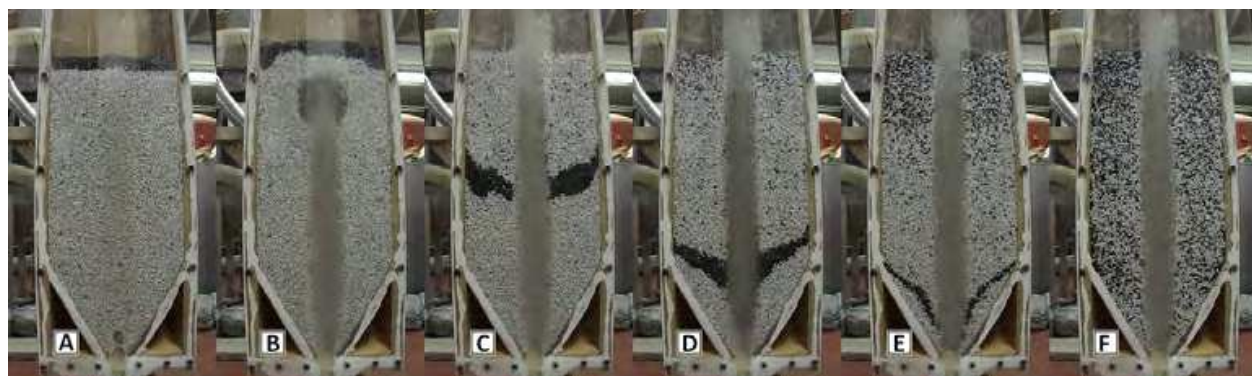


Fig. 15. The snapshot sequence indicates the motion of a tracer layer: A at  $t = 0$  s; B at  $t = 1$  s; C at  $t = 8$  s; D at  $t = 16$  s; E at  $t = 22$  s and F at  $t = 28$  s

annulus. The fifth image gives evidence of noticeable shear acting on the particles, though no internal mixing occurs as far as particles enter the spout; then, quite an amount of particles is thoroughly mixed in the spout and fountain as they begin recirculating. The last image indicates an overall good mixing condition.

Spout diameter and spout profile were measured at the flat transparent wall. The experimental mean values were compared against the predictions given in the literature (McNab, 1972), with a difference of about 10%, which indicates that squared-based spouted bed findings do match the ones obtained in cylindrical vessels.

## 9. Fluid dynamics of solids in multiple spouted beds and its modelling

One of the main goals of a spouted bed cascade is to control the mixing degree of the overall system and possibly generate a piston flow of the solid phase to guarantee identical residence time to all particles. These evaluations are carried out by means of stimulus-response techniques after attaining steady state in a continuously operating unit. Since each individual spouted bed appears to have about 90% of its volume in a perfectly mixed state (Epstein & Grace, 2011), the recycle ratio (ratio of internal circulation in the spout referred to feed rate) leaves a small volumetric fraction of the annulus to operate as plug flow. Residence time distribution (RTD) studies in multiple spouted bed were presented in the literature (Saidutta & Murthy, 2000) in small rectangular columns having two or three spout cells. The absence of internals in this system brought to fountain wandering and excessive fountain heights that caused overall mixing higher than the one corresponding to the number of mixed units in series. A detailed RTD study on stable systems and the correlation of the experimental results with respect to the ones predicted by a model can give a relevant contribution in designing these units. Models has gained increasing importance by making use of direct measurements in the half-sectional unit, thus becoming fully predictive.

### 9.1 Residence time distribution function

The RTD curves represent an effective way to interpret the fluid dynamics of the solid phase in a multiphase continuously operating reactor. These functions describe the elapse of time spent by individual solids fractions in the system and can be modelled by a relatively simple combination of ideal systems, each of them describing a basic element (mixed or plug flow system, dead zone, bypass, recycling).

Two types of curves can be studied. The  $E(t)$  function describes what a system releases instant after instant, i.e. the volumetric (or mass) fraction of particles whose residence time is between  $t$  and  $t+dt$ . The  $F(t)$  function provides the integral of  $E(t) \cdot dt$  and represents the fraction of elements whose residence time is lower than  $t$ .

The most direct way to trace an  $E(t)$  curve makes use of a physical tracer, whose characteristics are identical or very close to the ones characterizing the bulk of solids travelling the system. Usually, two types of stimulus are adopted, a pulse (given by a definite amount of tracer introduced into the system in the shortest time) or a step (an abrupt change from the normal feedstock to an identical feed made of tracer only). The first one is generally the prompter to use. Right away after the introduction of the pulse, samples are taken at the system exit with a proper scrutiny degree and the tracer concentration is measured and recorded.

The two  $E(t)$  and  $F(t)$  functions are defined below:

$$E(t) = \frac{C(t) \cdot \dot{M}}{M_{tr} \cdot \rho_b} \quad (5)$$

$$F(t) = \int_0^t E(t) dt \quad (6)$$

with  $C(t)$  being the concentration of solid tracer in the discharge,  $M_{tr}$  the mass of tracer injected,  $\rho_b$  the bulk density of tracer,  $\dot{M}$  the mass flow rate of solids travelling the system.

A pulse function (called Dirac function,  $\delta(t)$ ) is given by an instantaneous but finite entity (equal to unity) entering a system at  $t=0$ . The Laplace transforms of these functions allow the use of simple algebraic input/output relationships.

In our experiments, the pulse was obtained by quickly introducing in the feed a small amount of tracer (150 to 300 g, equivalent to about 1.5% of the total solids hold-up) made of PET chips doped with some ferromagnetic powder. After sampling the ferromagnetic PET chips were sorted out from the PET bulk by a magnet and their concentration calculated in each sample.

An example of RTD curves is given by Figure 16 which comparatively reports two  $E(t)$  curves obtained at steady state from tests in the 3-module spouted bed operated with and without submerged baffles, according to the configuration appearing on Figure 11B. The two curves overlap almost perfectly to demonstrate that internal baffles do not alter at all the solids circulation in a multi-unit cascade. The same test also demonstrates that the external solids streamlines do not have any transversal (horizontal) component, as also visible from half column monitoring. The slope of solids at the free surface was modest in these runs, due to a very low throughput (2 kg/min). Thus, it is straightforward assessing that batch operations do not require any repartition between modules. From these considerations, the use of submerged baffles is beneficial to the start-up phase of continuous processes only and becomes fundamental as geometrical boundary to generate the configuration given in Figure 12.

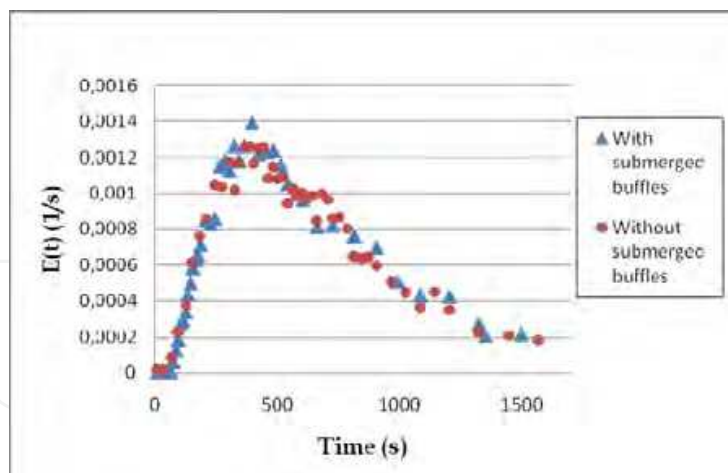


Fig. 16. Comparison between the RTD curves in the 3-module spouted bed with  $H/D_c=1.72$  with and without submerged baffles

## 9.2 Modelling

The theoretical description of continuous units combines basic elemental models, whose combination gives origin to a system capable of generating an overall response to properly match the actual behaviour of the real system studied. A descriptive model can produce an output without having a strict link with the actual hydrodynamic behaviour and then has to make use of fitting parameters. This approach does not allow sound predictions or extension to more complex reactor structures. A much powerful tool is produced by conceiving a phenomenological model based on experimental observations. These models become fully predictive since all parameters are based on actual measurements. Then, a model interacts with scale-up procedures through the validity of the correlations used rather than its structure.

Dynamic responses were obtained by making use of a Matlab Simulink tool by generating model schemes as given in the below Figures 17 and 18. The fundamental modelling was based on a one-stage spouted bed; a multiple-cell system was then given by a cascade of basic units.

### 9.2.1 Descriptive model

The initial modelling started by considering an early dynamic description of spouted beds, where the overall behaviour can be portrayed by a well-mixed system with a minor (8 to 10%) portion of plug flow. The corresponding scheme given in Figure 17 A) includes the feed rate  $F_1$ , the bypass to fountain  $F_3$  (which become negligible when the inlet diverting baffle is considered, as a consequence  $F_2 \equiv F_1$  and  $F_5 \equiv F_4$ ), the total circulation from spout  $F_4$ , the net discharge rate  $F_7 \equiv F_1$  (for continuity) and  $F_6 = F_4 - F_1$ . From the experimental conditions  $F_1$  is known and  $F_4$  can be estimated by measuring mean particle velocity at the frontal wall of half-column. As far as the other parameters than appear in Figure 17 B) are concerned,  $t_d$  is estimated from particle circulation,  $\tau_{annulus}$  follows from holdup in the annulus and  $\tau_{spout+fountain}$  is calculated by difference from the known bed holdup. At usual  $H/D_c$  ratios adopted in cylindrical columns, the ratio of these two time constants approaches one magnitude order.



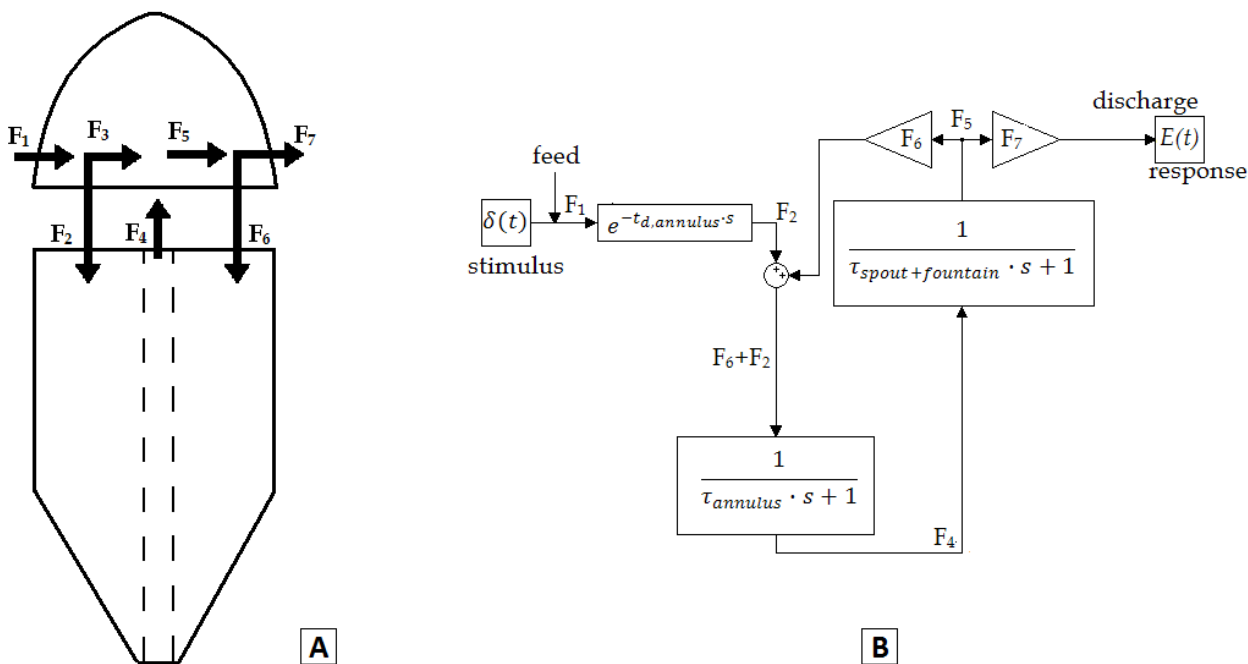


Fig. 17. Descriptive model of one stage two-zone continuously operating spouted bed: A): schematic of flow circulation between annulus and spout/ fountain regions; B) Simulink model including pulse stimulus, delay at annulus entrance, two perfectly mixed regions for annulus and spout/ fountain volumes and recirculation to bed surface.

Accepting this description also this model does not contain any fitting parameter, once the constitutive elements are assumed. Since the  $F_4$  (internal circulation) to  $F_7$  (net flow) ratio is very large, the overall system approaches a well-mixed unit and in this view the modelling is scarcely sensitive to the hydrodynamic description given to the annulus.

Figure 18 presents the comparison between experimental and modelling results for  $H/D_c = 1.72$ . The fitting is excellent, considering the time delay given by the minimum residence time of particles ( $t_d$ ) and the well-mixed key dynamic component brought by spout recirculation.

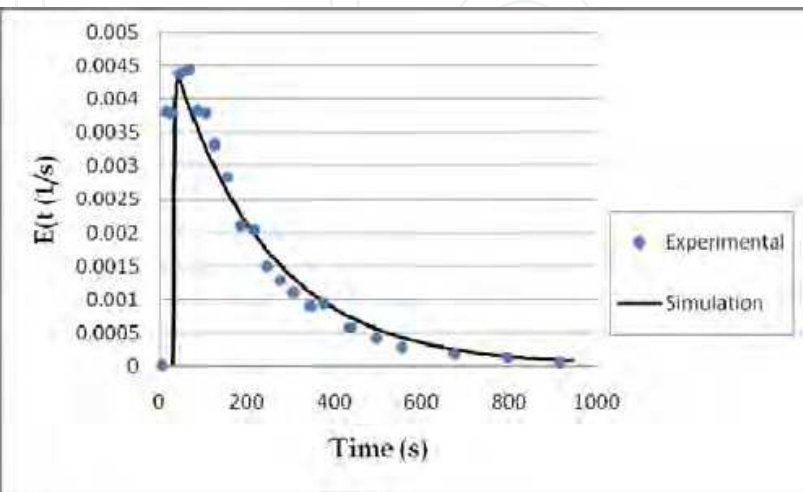


Fig. 18. Comparison between experimental data and the descriptive model

### 9.2.2 Phenomenological model

The relevant limitation contained by the above model consists in the fact that the annulus, representing the massive part of a spouted bed, has not been given a proper description. By observing it through the flat transparent wall of semicylindrical columns, particles show well-defined trajectories with scarce intermixing, according to consolidated findings (Mathur & Epstein, 1974).

The phenomenological description adopted in the updated model assumes that the squared-section of the annulus (with a cylindrical spout  $D_s$ ) is divided into three axisymmetric zones, each of them having the same width according to the scheme given in Figure 19 A). Each of these regions receives from the fountain a solids flow rate proportional to its cross sectional area ( $F_{6A}$ ,  $F_{6B}$  and  $F_{6C}$ , respectively moving from outside towards the spout). The flow fashion in each region is a piston with particle residence time  $t_{d,A}$ ,  $t_{d,B}$  and  $t_{d,C}$ , from the bed surface down to the cylinder-frustum junction, according to experimental observations. The mixing component acting in the annulus was concentrated in the frustum, which progressively discharges solids into the spout, depending on local streamline length. As a whole, this section was assimilated as far as its dynamics is concerned to a well-mixed volume, accounting to about 20% of the total holdup of the spouted bed. Also in this case, the effect of the  $F_4/F_7$  ratio overcomes the sensitivity of other variables on the model, so that the ratio between frustum to parallelepiped volumes (i.e. plug to well-mixed volume ratio) is not relevant at all.

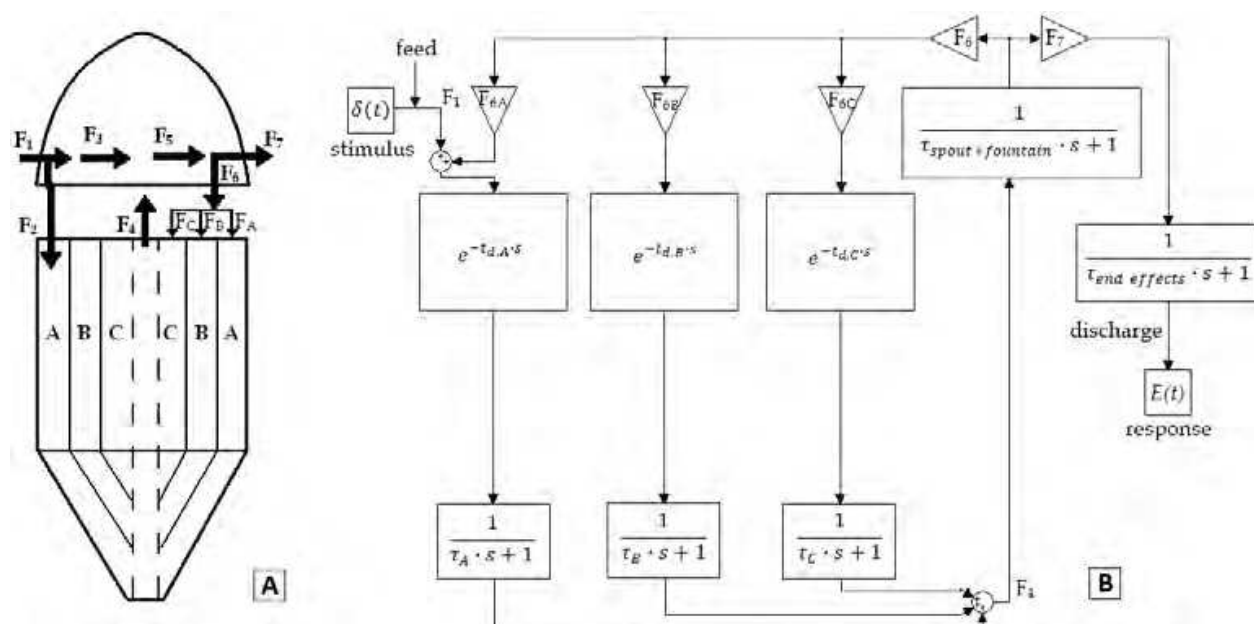


Fig. 19. Phenomenological model of one stage four-zone continuously operating spouted bed: A): schematic of flow circulation between annulus and spout/ fountain regions; B) Simulink model including pulse stimulus, three parallel delay times in annulus, followed by three perfectly mixed regions in bottom frustum, one perfectly mixed zone in spout/ fountain region and recirculation to bed surface. Small well-mixed volume accounts for sampling end effects.

Figure 19 B) presents the Matlab Simulink scheme, where the RTDF is generated by introducing the pulse into the sector A of the annulus (due to geometrical constrain of the



inlet baffle). The overall solids flow rate from fountain travels three parallel annulus pistons, then each portion of solids enters the corresponding well-mixed portion of frustum, respectively characterized by a mean residence time estimated by observations at the flat frontal wall. The spout collects particles from the annulus and mix them in the fountain. A small well-mixed volume characterizes the solids sampling operation to account for end effects.

Figure 20 compares experimental results to the output of the phenomenological model. Any difference can be hardly noted with respect to the previous descriptive model output. Due to plug flow effect, a certain oscillation matching the cycle time frequency is observed. A short sampling time  $\tau_{end\ effects}$  was sufficient to damp the greatest part of oscillation.

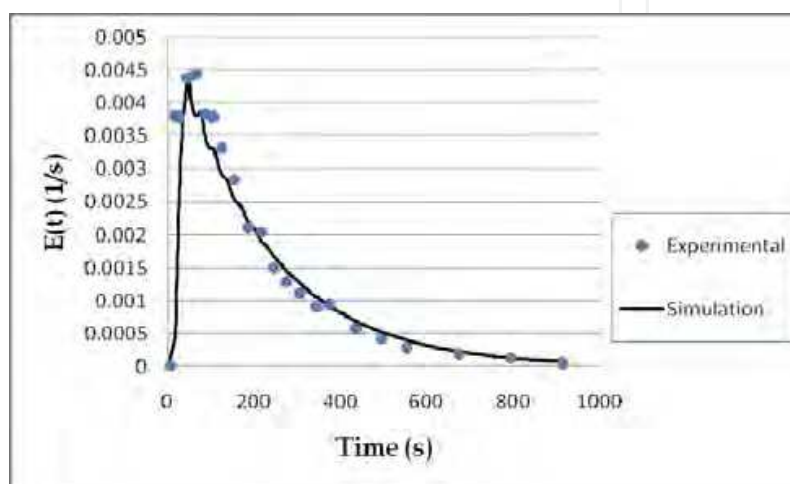


Fig. 20. Comparison between experimental data and the phenomenological model

### 9.2.3 Model validation for multiple units

The Matlab Simulink description conceived for the phenomenological model of one-stage spouted bed can be replicated a number of times corresponding to the number of cells included in a multistage system. An example is given in Figure 21 for a three-module

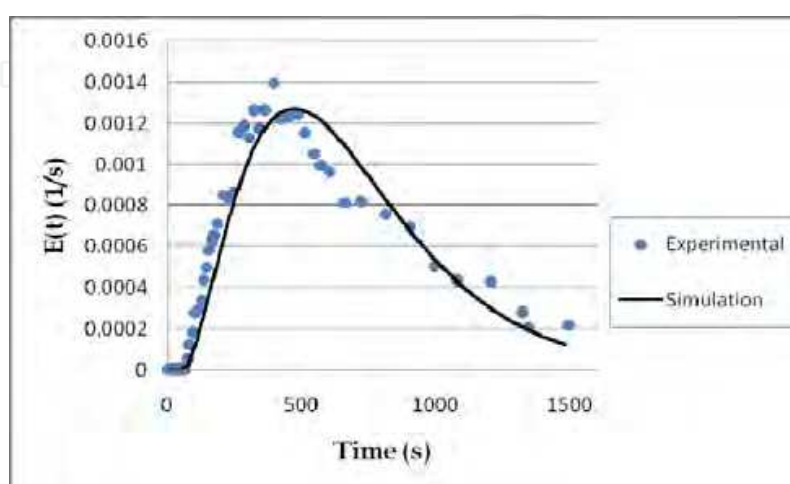


Fig. 21. Comparison between experimental and model RTDs in the 0.20 m side squared-based three-module spouted bed

spouted bed. The agreement is fully satisfactory, even though it may appear that experimental data anticipate the model output moderately and then a tail slightly higher than expected is displayed. This analysis could require to consider some direct bypass from fountain to downstream stage through the gap between submerged and freeboard vertical baffles and a small partially stagnant backwater, possibly existing along edges of frustum walls.

## 10. Final remarks on multiple bed start-up and shut-down

Both cold tests on the dual and triple module square-based spouted beds and industrial operations on the sextuple module demonstration unit (Beltramo et al., 2009) show that design criteria, operating conditions and step sequence must be defined carefully. In opposite case, start up and transitory from spouting onset in one module to overall stable spouting might be a serious issue. The key design parameters affecting start-up are:

- Cross-sectional area of the gap between vertical baffles: it should be designed to allow a maximum solids flow rate equal to the process solids nominal capacity with an excess of about 50% to avoid solids flooding (if too narrow) or bed emptying (if too large, because of direct discharge from fountain).
- Freeboard baffle height: it has to fully cover the fountain height at spouting onset and, if the structure of an industrial unit is considered, should reach the top deflectors of particles to avoid upper solids bypass.
- Cross-section of particle deflectors on gas phase path in each module (in the upper part of freeboard, above fountain projections): it has to be designed to set a progressive decrease of gas cross-sectional velocity and avoid any upward solids elutriation.
- The design of pyramid frustum base should consider a small gap between the orifice circumference and the slanted wall to help particle circulation. This gap is related to the average size of particulate material with a factor larger than 2. Several experiments have demonstrated that in case of local stagnation at the frustum bottom, this dead zone may spread up to the pyramid/parallelepiped junction. A careful bottom design and/or high gas flow rate counter this undesired phenomenon.
- Spouting modules have to be assembled at sufficient different elevation to guarantee a steady and even solids holdup. A rule of thumb drawn from experimentation suggests that  $\Delta H \approx 0.5 D_c$  surely gives origin to a non-interacting system and prevents bed emptying of downstream modules, or vice versa avoid extra hold up in upstream ones.
- Each module must be provided of independent gas flow regulation.

Given the fact that gas phase pressure drop is maximum at incipient start-up (up to 2 to 3 times of the gas pressure drop at stable spouting for conical or cylindrical shallow beds), to avoid oversize of circuit blower, with consequential dramatic increase of capital and operating costs, one can proceed according to two start up routes:

- a. **Start-up with reduced solids holdup:** fill the first module with 1/3 to 1/2 depth with respect to the design bed load; start injecting gas till fountain formation, then begin filling the bed to reach the operating solids bed depth and then continue feeding solids at nominal flowrate to reach overflow discharge to the second module. Continue with the same procedure for all modules.

- b. **Start-up with full solids holdup:** fill each module with the design solids bed depth, provide the circuit with a capacitive booster section, suitable to inject high pressure gas to bed orifices for about 10 to 15 seconds and reach external spouting onset; then operate spouting process with the master circuit blower.

In a multiple-bed spouting unit, to have the whole series of spouted beds started up, one has to proceed with a start-up sequence, one by one, from the first bed to the last one, following the solids flow direction. Monitoring the gas phase pressure drop vs. time represent the trigger element for the control system to determine when the start-up of one module is completed and the situation is ready to move and start up next module. The b) procedure is safer since enough head is available to re-start the system in case of failure.

The above defined key design parameters are also suited for shutdown phase. As far as this procedure is concerned, one has to stop solids feeding, allowing holdup of each module to be processed at the steady state operating conditions (as to minimize off-spec), while decreasing each bed depth to a level lower than the overflow weir. At that point, side submerged baffles must be risen, while gas flow continues to be injected to each bed, so to have prompt residual solid emptying.

## 11. Conclusions

Spouted beds, throughout over half a century studies, have demonstrated to display very interesting features against bubbling conventional fluidization. Thanks their peculiar hydrodynamic structure a relevant gas rate can be saved also operating at the maximum spoutable bed depth. Again, the total frictional pressure drop across a spouting unit can be as lower as one-third of the one in a corresponding particulate material fluidization. The application of spouted bed to relatively coarse solids overcomes undesirable features characteristic of fluidization, namely random gas channelling and solids circulation, slugging and poor contacting between phases.

The scale-up issue of spouting units has remained open since their initial invention and the debate on whether prefer larger or multiple units has struck the opinion of scientists and technologists every time that this problem required a sound solution. This chapter has tackled the scale-up problem by opting for a square-based spouted bed geometry, since constructing a cascade of these vessels is economically advantageous and much more effective for the solids fluid dynamics as well as for insulation problems.

Following the experience gained during an industrial demonstration project, encouraging results came by evaluating the product quality; the potential performance of a multiple spouted bed was thus confirmed. Nevertheless, this unit required an excessive attention to govern its stability over time and the need of several improvements was highlighted.

A new research project required the construction of several apparatuses to pursue a comprehensive strategy which has aimed at:

- comparing the fundamental operating parameters of square-based spouted beds with the corresponding values characteristic of conventional cylindrical columns,
- carrying out an adequate experimental scale-up,

- demonstrating the achievement of fully stable operations by introducing novel concepts (stage segregation with internal baffles, sloped cascade of stages) in designing a multi-cell equipment,
- obtaining a plug flow of solids with a sufficient number of stages, which may implement process scale-up at the same time,
- modelling single unit and multiple square-based spouted beds to predict solids hydrodynamics.

The final structure of a cold model apparatus has demonstrated the achievement of all the listed goals.

## 12. Acknowledgments

The economical support granted by ENGICO Srl (LT- Italy) allowed construction of the equipment and the research fellowship to one of the authors (M. C.). The authors wish to thank Mr. Alfio Traversino for patiently and carefully constructing the three-module experimental rig.

## 13. Nomenclature

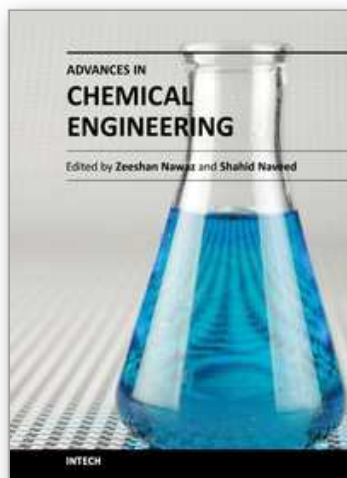
$Ar$	Archimedes number
$C$	concentration of solid tracer in the discharge, kg / m <sup>3</sup>
$D_c$	column diameter, m
$d_i$	inlet diameter, m
$d_p$	particle diameter, m
$D_s$	mean spout diameter, m
$E(t)$	E function
$F(t)$	F function
$H$	bed depth, m
$H_m$	maximum spoutable bed depth, m
$\Delta H$	gap between adjacent units, m
$\dot{M}$	mass flow rate of solids, kg / s
$M_{tr}$	mass of the tracer, kg
$\Delta P_M$	maximum pressure drop across bed, Pa
$\Delta P_S$	spouting pressure drop across bed, Pa
$U$	fluid velocity, m / s
$U_{ms}$	minimum spouting velocity, m / s
$U_{onset}$	fluid onset velocity, m / s

Greek letters:

$\alpha$	free surface slope, deg
$\delta(t)$	Dirac function
$\lambda$	shape factor
$\rho_f$	fluid density, kg / m <sup>3</sup>
$\rho_b$	bulk solids density, kg / m <sup>3</sup>
$\rho_s$	actual material density, kg / m <sup>3</sup>
$\tau$	mean residence time, s

## 14. References

- Beltramo, C.; Rovero, G. & Cavaglià, G. (2009). Hydrodynamics and thermal experimentation on square-based spouted beds for polymer upgrading and unit scale-up. *The Can. J. Chem. Eng.*, Vol.87, 394-402
- Cavaglià, G. (2003), "Reactor and process for solid state continuous polymerisation of polyethylene terephthalate (PET)" Patent EP 1576028 B1
- Chatterjee, A. (1970). Spout-fluid bed technique. *Ind. Eng. Chem. Process Des. Develop.*, Vol.9, 340-341
- Epstein, N. & Grace, J. (2011). *Spouted and spout-fluid beds*. Cambridge Univ. Press, ISBN 978-0-521-51797-3, New York
- Gishler, P.E. & Mathur, K.B. (1957). Method of contacting solid particles with fluids. U.S. Patent No. 2,786,280 to National Research Council of Canada
- Grbavčić, Ž.B.; Vuković, D.V.; Hadžismajlović, D. E.; Garić, R. V. & Littman, H. (1982). Fluid mechanical behaviour of a spouted bed with draft tube and external annular flow. *2<sup>nd</sup> Int. Symp. on Spouted Beds, 32<sup>nd</sup> Can. Chem. Eng. Conf.*, Vancouver, Canada
- Geldart, D. (1973). Type of gas fluidization. *Powder Tech.*, Vol.7, 285-292
- Malek, M.A. & Lu, B.C.Y. (1965). *I&EC Process. Des. Develop.*, Vol.4, 123-127
- Mathur, K.B. & Epstein, N. (1974). *Spouted beds*, Academic Press, ISBN 0-12-480050-5, New York
- McNab, G.S. (1972). Prediction of spout diameter. *Brit. Chem. Eng & Proc. Techn.*, Vol.17, 532
- McNab, G.S. & Bridgwater, J. (1977). Spouted beds – estimation of spouting pressure drop and the particle size for deepest bed. *Proc. of European Council on Particle Technology*, Nuremberg, Germany
- Metcalf, J. R. (1965-66). The mechanics of the screw feeder. *Proc. Inst Mech. Eng.*, Vol.180, 131-146
- Murthy, D.V.R. & Singh, P.N. (1994). Minimum spouting velocity in multiple spouted beds. *The Can. J. Chem. Eng.*, Vol.72, 235-239
- Piccinini, N. (1980). Particle segregation in continuously operating spouted beds, In: *Fluidization III*, J.R Grace & J.M. Matsen, (Eds), 279-285, Plenum Press, ISBN 0-306-40458-3, New York, USA
- Rovero, G.; Piccinini, N. & Lupo, A. (1985). Vitesses des particules dans les lits à jet tridimensionnel et semi-cylindriques. *Entropie*, Vol.124, 43-49
- Saidutta, M.B. & Murthy, D.V.R. (2000). Mixing behavior of solids in multiple spouted beds. *The Can. J. Chem. Eng.*, Vol.78, 382-385



## **Advances in Chemical Engineering**

Edited by Dr Zeeshan Nawaz

ISBN 978-953-51-0392-9

Hard cover, 584 pages

**Publisher** InTech

**Published online** 23, March, 2012

**Published in print edition** March, 2012

Chemical engineering applications have been a source of challenging optimization problems in terms of economics and technology. The goal of this book is to enable the reader to get instant information on fundamentals and advancements in chemical engineering. This book addresses ongoing evolutions of chemical engineering and provides overview to the state of the art advancements. Molecular perspective is increasingly important in the refinement of kinetic and thermodynamic modeling. As a result, much of the material was revised on industrial problems and their sophisticated solutions from known scientists around the world. These issues were divided into two sections, fundamental advances and catalysis and reaction engineering. A distinct feature of this text continues to be the emphasis on molecular chemistry, reaction engineering and modeling to achieve rational and robust industrial design. Our perspective is that this background must be made available to undergraduate, graduate and professionals in an integrated manner.

### **How to reference**

In order to correctly reference this scholarly work, feel free to copy and paste the following:

Giorgio Rovero, Massimo Curti and Giuliano Cavaglià (2012). Optimization of Spouted Bed Scale-Up by Square-Based Multiple Unit Design, *Advances in Chemical Engineering*, Dr Zeeshan Nawaz (Ed.), ISBN: 978-953-51-0392-9, InTech, Available from: <http://www.intechopen.com/books/advances-in-chemical-engineering/optimization-of-spouted-bed-scale-up-by-square-based-multiple-unit-design>

**INTECH**  
open science | open minds

### **InTech Europe**

University Campus STeP Ri  
Slavka Krautzeka 83/A  
51000 Rijeka, Croatia  
Phone: +385 (51) 770 447  
Fax: +385 (51) 686 166  
[www.intechopen.com](http://www.intechopen.com)

### **InTech China**

Unit 405, Office Block, Hotel Equatorial Shanghai  
No.65, Yan An Road (West), Shanghai, 200040, China  
中国上海市延安西路65号上海国际贵都大饭店办公楼405单元  
Phone: +86-21-62489820  
Fax: +86-21-62489821



© 2012 The Author(s). Licensee IntechOpen. This is an open access article distributed under the terms of the [Creative Commons Attribution 3.0 License](https://creativecommons.org/licenses/by/3.0/), which permits unrestricted use, distribution, and reproduction in any medium, provided the original work is properly cited.

IntechOpen

IntechOpen